Competitiveness and synergy between three flame retardants in poly(ethylene-co-vinyl acetate)

Henri Vahabi, Amin Raveshtian, Mohammad Fasihi, Rodolphe Sonnier, Mohammad Reza Saeb, Loïc Dumazert, Baljinder K. Kandola

Competitiveness and synergy between three flame retardants in poly(ethylene-*co*-vinyl acetate)

Henri Vahabi [a, *], Amin Raveshtian [b], Mohammad Fasihi [b, **], Rodolphe Sonnier [c], Mohammad Reza Saeb [d], Loïc Dumazert [c], Baljinder K. Kandola [e]

[a] *Université de Lorraine, Laboratoire MOPS E.A. 4423, Metz F-57070, France*
[b] *School of Chemical Engineering, Iran University of Science and Technology, Tehran 16846-13114, Iran*
[c] *Centre des Matériaux des Mines d'Alès (C2MA) - 6, Avenue de Clavières 30319 Alès Cedex, France*
[d] *Department of Resin and Additives, Institute for Color Science and Technology, P.O. Box: 16765-654, Tehran, Iran*
[e] *Institute for Materials Research and Innovation, University of Bolton, Bolton BL3 5AB, United Kingdom*

A B S T R A C T

This work seeks to address the effect of simultaneous use of three flame retardants, having three different modes of action, (magnesium hydroxide, expanded and expandable graphite) on the thermal degradation and flame retardancy of poly(ethylene-co-vinyl acetate). Thermal conductivity of samples was measured in order to investigate the effect of the use of expanded and expandable graphite on the time-to-ignition and the peak of heat release rate in cone calorimeter test. Thermal shielding performances of chars were studied as well. It was found that there is an optimum ratio between expanded and expandable graphite in order to control thermal conductivity and therefore fire properties. Some correlations were also found between the char thickness and the first peak of heat release rate.

Keywords:
Poly(ethylene-*co*-vinyl acetate)
Magnesium hydroxide
Graphite
Flame retardancy
Thermal conductivity

1. Introduction

Poly(ethylene-co-vinyl acetate) (EVA) copolymer has been widely used in a variety of areas such as cable and wire insulation, adhesive, solar energy, construction, and packaging industries [1,2]. However, EVA is known as a highly flammable polymer. The fire behavior of EVA has been extensively studied over recent years. In this regard, the effect of different "additive flame retardant" systems on the flame retardancy of EVA has been investigated [3–11]. Among flame retardants incorporated into EVA, metallic hydroxides, magnesium hydroxide (MDH) and alumina trihydrate (ATH) have been comprehensively studied in view of their exceptional efficiencies. The mechanism of action of MDH is similar to that of ATH consisting of an endothermic reaction, through release of water followed by formation of a protective mineral layer (MgO and Al_2O_3) on the surface of polymer during the course of combustion. Fire properties of EVA were significantly governed by the individual and/or simultaneous use of MDH and ATH.

The combination of MDH or ATH with different flame retardants has also been examined to attain synergistic effects on fire properties of EVA. This strategy allows decreasing the incorporation level of flame retardant in EVA, and thus improving mechanical properties. Almost all additives have been considered, most often to improve the cohesion of the mineral barrier formed by the accumulation of alumina or magnesium oxide on the top surface of the composite during combustion. The cohesion of the formed residue during combustion, which is of crucial importance in cable and wire insulation applications, as well as its thickness more or less determine the flame retardancy properties [12–14]. For example in cable industry, the NFC 32070 CR1 standard test imposes that cables sustain electrical power where jackets must protect the copper [15,16]. Generally, synergist is used at 1–5 wt.%, but in some cases higher contents (>10 wt.%) are used. Zinc, calcium or melamine borate [17–22], montmorillonite [9,23–30], talc [11,20], silica and silicon-based fillers [31–34], layered double hydroxide [35], and carbon nanotubes [23,36] have been considered in this context.

Expandable graphite (EG), also known as intumescent flake

* Corresponding author.
** Corresponding author.
E-mail addresses: henri.vahabi@univ-lorraine.fr (H. Vahabi), mfasihi@iust.ac.ir (M. Fasihi).

graphite, is a form of intercalated graphite used to promote intumescence and efficiency of barrier layer during burning in EVA [37–39]. Expanded graphite (EDG) generally assists in heat dissipation on the surface of the polymer, and therefore delays the increase in surface temperature [40,41]. It has been observed that Time-To-Ignition (TTI) increases when EDG is incorporated into a polymer [42]. However, the increase in TTI could be counterbalanced by the acceleration of the Heat Release Rate (HRR); and consequently an increased HRR peak, as reported by Patel et al. [43]. Such phenomena were explained by heat transfer from the surface to the bulk of sample. It was observed that TTI increases because of the increase in the thermal conductivity of polymer in the presence of heat conductor additive as EDG, followed by a fast heating of the bulk leading to a rise in pHRR [44,45]. Despite such a history behind the use of EDG as an efficient flame retardant, to the best of the knowledge of authors of this work, its synergistic potential in combination with MDH or ATH has not been examined yet.

The present work aims to (*i*) investigate the combination effect of three different flame retardants (MDH, EG and EDG) each one providing their own action towards fire properties improvement of EVA; (*ii*) the competiveness and/or synergy between EG and EDG and their simultaneous influence on two crucial parameters, TTI and intumescence, as well as thermal conductivity, Scheme 1. The efficiency of hybrid flame retardant systems developed in this work, which contains different amounts of MDH, EG, and EDG was assessed using a complete set of experiments performed on composite samples including microscopy, thermogravimetric analysis, thermal conductivity, and cone calorimetry analyses.

2. Experimental

2.1. Materials

Ethylene vinyl acetate copolymer, EVA 1316 (MFI = 0.8 g/10min; vinyl acetate content = 18 wt.%), was purchased from Hanwa Chemical, South Korea, and used as matrix. Three types of fillers were used as flame retardants: Magnesium dihydroxide (MDH) was purchased from Daejung Chemicals & Metals Co. Ltd, South Korea, while expandable graphite (EG) (expansion ratio = 200 cc.g^{-1}; particle size > 300 μm) and expanded graphite (EDG) (average particle size = 100 μm) were both obtained from Ito Kokuen Co., Japan.

2.2. Sample preparation

EVA and flame retardants were mixed in a batch melt mixer (Brabender W50 EHT) at 150 °C and a rotor speed of 80 rpm. First, EVA was fed into the mixing chamber and after melting, MDH, expanded and expandable graphite were added to the mixer, respectively. The total mixing time for all samples was fixed at 10 min. Neat EVA was prepared under the same condition, for comparison. The samples nomenclature and composition are given in Table 1. After the melt mixing completed, the samples were compression-molded at 180 °C under 10 MPa for 10 min in a square 100 mm × 100 mm × 4 mm mold.

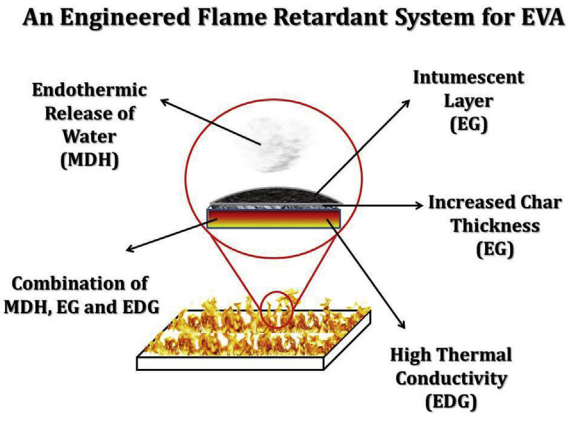

Scheme 1. Contribution of MDH, EDG and EG to flame retardancy of EVA.

2.3. Instrumentation

Morphology of composites was observed by a scanning electron microscope (FEI Quanta 200 SEM). All micrographs were obtained under high vacuum at a voltage of 10 kV with a spot size of 4 and a working distance of 8–10 mm. Small bars of EVA composites were cryofractured in the liquid nitrogen into two pieces. Prior to microscopic measurements, the cryofractured surfaces were sputter coated with carbon to make them conductive.

Thermal decomposition was investigated using a Setaram Labsys Evo thermogravimetric analyzer. All measurements were performed under nitrogen with a heating rate of 10 °C.min^{-1}. The sample weight was 30 ± 2 mg. Cone calorimeter tests were performed on 100 × 100 × 4 mm^3 sheets using an incident heat flux of 50 kW m^{-2}, according to ISO 5660. Peak of Heat Release Rate (pHRR), Total Heat Release (THR), Total smoke production (TSP), and Time-To-Ignition (TTI) were recorded from this test. Three experiments were performed for each sample. Accuracy is estimated to be around 5%. The appearance of the residual chars after the cone calorimeter tests was observed by a digital camera to assess the intumescence and char integrity.

Thermal diffusivity α (m^2.s^{-1}) was measured using a Laser Flash apparatus (XFA600 from Linseis). The specimens were stamped from compression-molded 100 × 100 × 4 mm^3 sheets, thinned to a thickness of 2 mm and coated with graphite on both surfaces. Measurements were carried out at room temperature in vacuum.

Thermal diffusivity, α is closely related to thermal conductivity, known as the equation (1):

$$\alpha = \lambda/\rho c \quad (1)$$

Thermal conductivity was calculated using typical values of density ρ and specific heat c. These values can be found in the literature for EVA and fillers. These values are shown in Table 2. Even if thermal conductivity changes during burning, the measurement of its initial value is useful to understand the changes in time-to-ignition.

Table 1
Name and composition of the samples prepared in this study.

Sample code	EVA (wt.%)	MDH (wt.%)	EDG (wt.%)	EG (wt.%)
E100	100	0	0	0
EM-50	50	50	0	0
EM-45	50	45	5	0
EM-40	50	40	10	0
EM-35	50	35	15	0
EM-30	50	30	20	0
EME-15	50	30	15	5
EME-10	50	30	10	10
EME-5	50	30	5	15
EME-0	50	30	0	20

Table 2
Density and specific heat for EVA and fillers used to calculate thermal conductivity.

	Density ($g.cm^{-3}$)	Specific heat ($J.g^{-1}.K^{-1}$)	References
EVA	0.94	1.4	[46,47]
MDH	2.34	1.33	[48,49]
EDG	2.25	0.7	[50,51]
EG	1.5	0.7	[48,52]

3. Results and discussion

3.1. Morphology observations

The dispersion states of flame retardants in EVA were monitored by SEM. Fig. 1 provides SEM images for four samples containing MDH (EM-50, Fig. 1a), MDH/EDG (EM-30, Fig. 1b), MDH/EDG/EG (EME-10, Fig. 1c), and MDH/EG (EME-0, Fig. 1d). The micronic particles of MDH were regularly dispersed in EVA with sizes below 1 μm. However, the presence of aggregates was also observed, Fig. 1a. The image of EM-30 sample showed the presence of EDG platelets and also MDH with the same dispersion state as previously observed for EM-50. The thickness of graphite sheets was nanometric, Fig. 1 b. The difference in dispersion between EG and EDG and the form of EG was not clear from Fig. 1c. However regarding Fig. 1 d, it seems that EG "particles" are platelets roughly similar to EDG.

3.2. Thermogravimetric analysis (TGA)

Fig. 2 shows the TGA curves of MDH, expanded graphite and expandable graphite. The dehydration decomposition of MDH was in the range of 330–460 °C, and the residual mass was 68%. Expanded graphite was thermally stable until 800 °C. Expandable graphite loses about 10% of its weight since 190 °C due to release of volatile gases from the intercalant at this temperature [53,54]. Fig. 3 and Fig. 4 present the TGA curves of EVA and EVA-based composites. The obtained parameters from these curves are summarized in Table 3. EVA and all composites showed a two-step weight loss. In the first decomposition step, from 300 to 380 °C, EVA loses acetic acid and carbon-carbon double bonds are formed along the polymer backbone [55,56]. The dehydration reaction of MDH was simultaneously performed in this range. The second degradation step, from 430 to 500 °C, is attributed to the chain scission of the polymer and the volatilization of the residue [8,57].

The thermal stability of composites was superior to that of pure EVA. The onset temperature of degradation (first step) increased from 303 °C for EVA to 322 °C for EM-50 and to about 316 °C for other composites. However, the mixtures of MDH and expanded graphite or expandable graphite were less effective than pure MDH in improving the thermal stability of composites. In the composites including expandable graphite, it was expected that the expansion of this filler during heating forms a protective layer against the heat which improved thermal stability. Nevertheless, it seems that this mechanism is not effective for the very small samples such as the ones used in TGA test. The residue at 600 °C increased from 37.5 wt.% for EM-50 to 39, 44 and 46 wt.% for EM-40, EM-30, and EME-10. This implies that the expanded graphite and expandable graphite may promote charring.

3.3. Cone calorimeter

The heat release rate (HRR) curves as a function of time are presented in Fig. 5 (samples containing MDH and EDG) and Fig. 6 (samples containing MDH, EDG, and EG). The obtained parameters from these curves (TTI, pHRR, TSP, THR) are summarized in Table 4. The peak of HRR (pHRR) decreased to 360 kW m^{-2} when

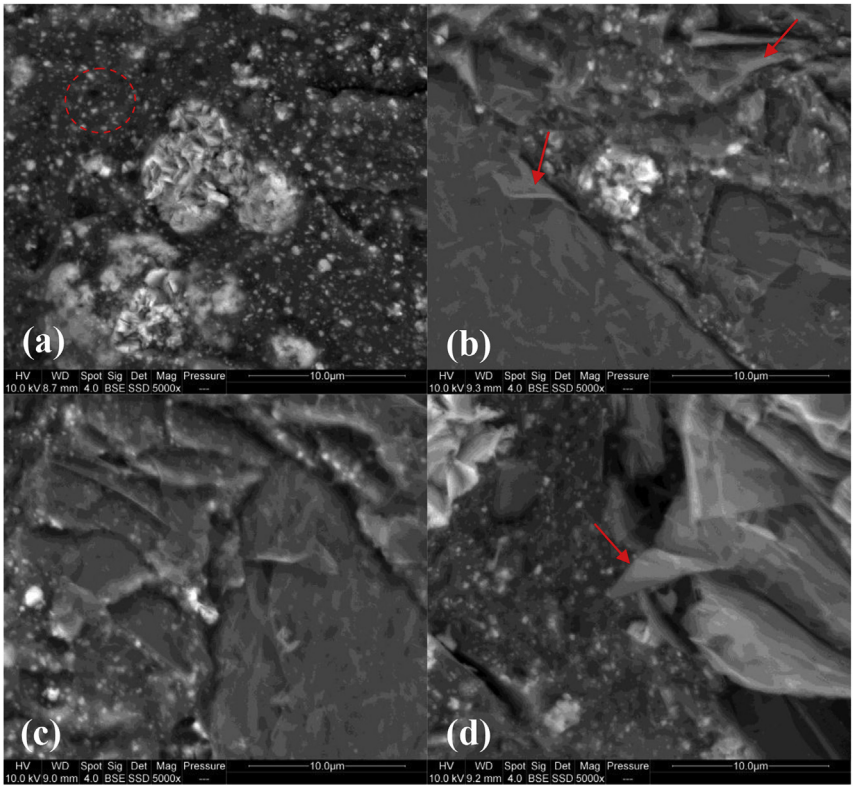

Fig. 1. SEM images of a) EM-50, b) EM-30, c) EME-10, and d) EME-0 samples.

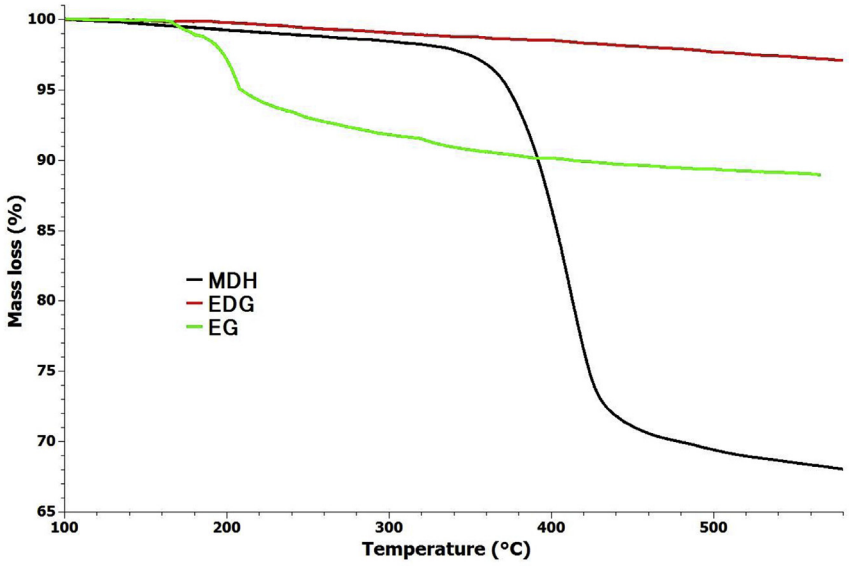

Fig. 2. TGA curves of MDH, EDG and EG, at heating rate of 10 °C.min^{-1} under nitrogen.

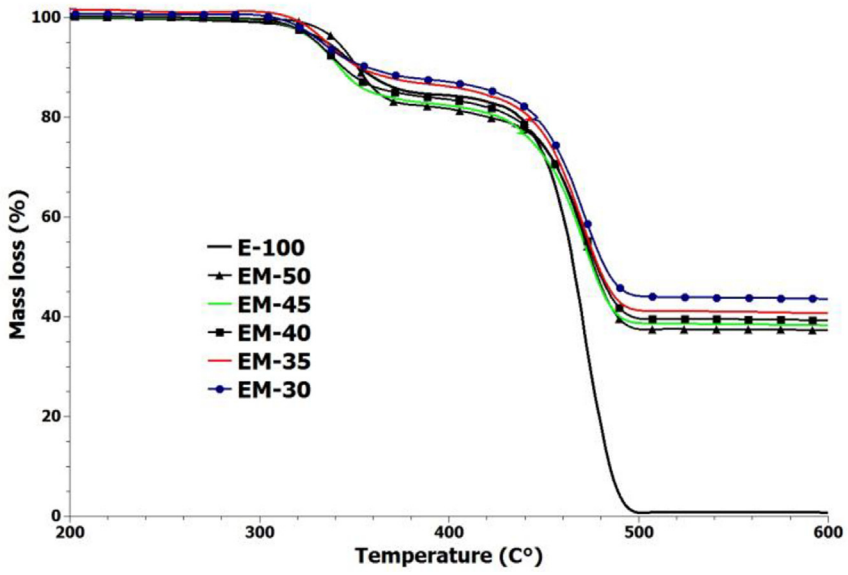

Fig. 3. TGA curves of all EM and E-100 samples, at heating rate of 10 °C.min^{-1} under nitrogen.

MDH was added to EVA. This represents a reduction of 74% of pHRR compared to pure EVA (1350 kW m^{-2}). The TTI was shifted to 110 s for this sample. The combination of MDH and EDG led to the decrease in pHRR and to the increase in TTI, Fig. 5. Regarding the shape of curves, two behaviors can be distinguished. In the case of EM-45 sample, a first peak appeared at 220 s, and then a second peak at 515 s. This behavior has already been explained by Schartel and Hull [58] as the evidence of thermally thick charring materials. They claimed that the appearance of the second peak was due to cracking and to the release of flammable gases during combustion. When the rate of EDG increased in the blend, TTI increased and the trough between two peaks decreased, from EM-45 to EM-30. It was also observed that pHRR decreased by the increase in EDG rate. However, second pHRR increased at 15 and 20 wt.% of EDG loading (EM-35 and EM-30 samples) compared to the samples containing only 5 and 10 wt.% of EDG. The second peak totally disappeared for these samples. The disappearance of the second peak may be explained by the reinforcement of char residue with an increase in the rate of EDG for EM-30 sample. Obviously, EM-40 sample (containing 40 wt.% MDH and 10 wt.% EDG) gives the best results among samples of this kind. The HRR peak for this sample was 242 kW m^{-2}. It could therefore be concluded that there is an optimal combination rate between EDG and MDH.

The substitution of 5 wt.% of EDG with EG led to the decrease in pHRR and re-appearance of a second peak at 413 s, Fig. 6. Afterwards, by adding EG, the pHRR decreased and the shape of curves was changed. However, TTI decreased by increasing the loading rate of EG. The comparison of HRR curves of EM-30 and EME-0 samples, Fig. 7, shows that the combination of MDH and EG is more efficient than that of MDH and EDG, in terms of flame retardancy. The decrease in pHRR for EME-0 was 90.4%, compared to pure EVA. However, the TTI was much higher in the case of EM-

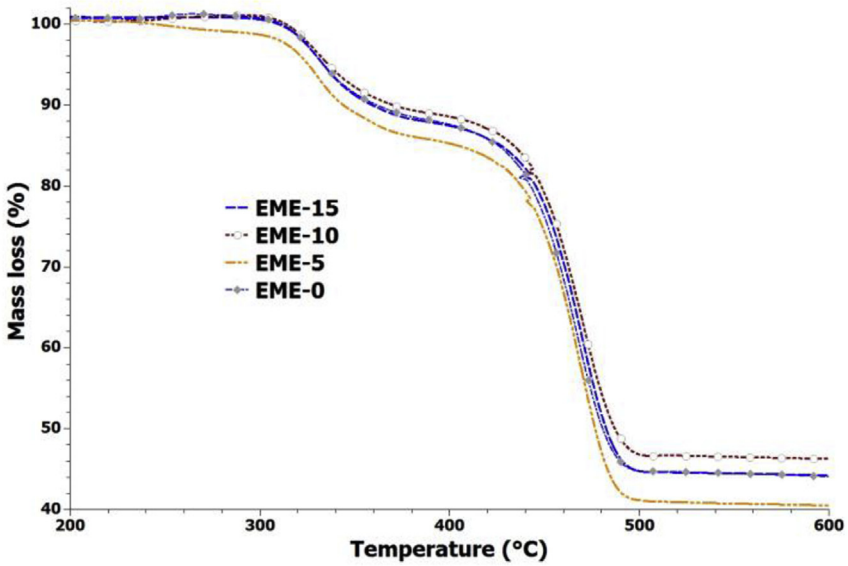

Fig. 4. TGA curves of EME samples, at heating rate of 10 °C.min^{-1} under nitrogen.

Table 3
TGA parameters for all samples, collected from TGA curves, under nitrogen ($T_{10\%}$ is temperature at 10% weight loss, T_{max} is the maximum rate degradation temperature, from DTG.).

Sample code	$T_{10\%}$ (°C)	T_{max} (°C)	Residue (wt.%) at 600 °C
MDH	391	402	68
EDG	–	322	97
EG	410	230	89
E100	352	345–473	0.7
EM-50	351	351–472	37.5
EM-45	341	340–472	38.5
EM-40	344	341–471	39
EM-35	352	336–471	41
EM-30	356	334–471	44
EME-15	359	332–471	44
EME-10	369	332–471	46
EME-5	343	332–470	40.5
EME-0	361	331–468	44

30 sample (combination of MDH and EDG).

Total smoke production (TSP) was also determined with cone calorimeter test. All TSP curves were shown in Fig. 8. The total smoke production of EME-0 and EME-5 sample was significantly reduced (black arrow). For the second group of samples, the TSP tended to reach a steady state after 550 s (red arrow). For the third group of samples (purple arrow), TSP increased steadily. It may be concluded that char barrier was more efficient in the case of the first two groups, and that the acceleration of TSP for the third group (purple arrow) was due to the non-effectiveness barrier character of their residues.

The images of residues after cone calorimeter test are presented in Fig. 9. Three forms of residue were observed after test. In the case of EM-50 sample, a brittle and thin residue was formed. For the samples containing both MDH and EDG, the char surfaces were smooth. However, the inside of char was porous, with large holes. The residues of samples containing EG were compact, dense, with a "worm-like"roughened surface, and without internal porosity. Char thickness values, Table 4, was increased by increasing the rate of EDG or EG, except for EME-15 samples. The addition of EG at 15 to 20 wt.% allowed to considerably promote the formation of an expanded char residue, which prevented the heat and gas transfer between the flame zone and the burning substrate, and thus limited the heat release.

Fig. 10 shows SEM images of EM-40 and EME-10. Two types of texture could be observed for all samples. The samples containing MDH and EDG present a smooth char surface, Fig. 10 a. The char surface of samples containing MDH, EDG and EG are more porous and contain the worm-like structure which is formed during the expansion of EG Ref. [59], Fig. 10 b.

The three fillers contribute to the barrier effect by accumulating at the top surface of the sample. Moreover, intumescence is promoted especially by expandable graphite. It is always challenging to correlate fire performances including pHRR occurring just after ignition to final residue morphology. However if the barrier layer develops early during the test, such correlations make sense. Fig. 11 shows the change in first pHRR versus char thickness. E100 was not considered because the amount of fuels is different from other samples and no char is formed. First pHRR seems to decrease continuously when thickness of the char at the end of the test increases. For EM samples containing 10, 15 and 20 wt% of EDG, the char thickness is almost the same but the pHRR increases when the EDG content increases. As already discussed, this change can be related to the high thermal conductivity which promotes the heat transfer to bulk leading to higher heat release rate.

Fig. 12 shows the change in THR versus the char thickness. Up to 25 mm-thick, char is not protective enough to avoid complete pyrolysis of EVA. Therefore THR is constant and close to 19.5 kJ/g. Thicker chars obtained with 15 and 20 wt% of EG limits the heat transfer so that EVA is not fully pyrolysed. THR of EME-0 is only 13.8 kJ g^{-1}, i.e. only 70% of the heat released in case of complete pyrolysis of EVA (19.5 kJ g^{-1}). These results highlight the huge effect of intumescent residue to improve the flame retardancy.

3.4. Study of heat transfer in composites

Time-to-ignition in cone calorimeter test, changes from 65 to 130 s according to the composite, Table 4. The three fillers used in this study have different impacts on TTI. Ignition occurs when the surface temperature reaches a critical value. A couple of phenomena influence the heating of the material during the pre-ignition period. The significant increase in TTI when 50 wt.% of MDH are

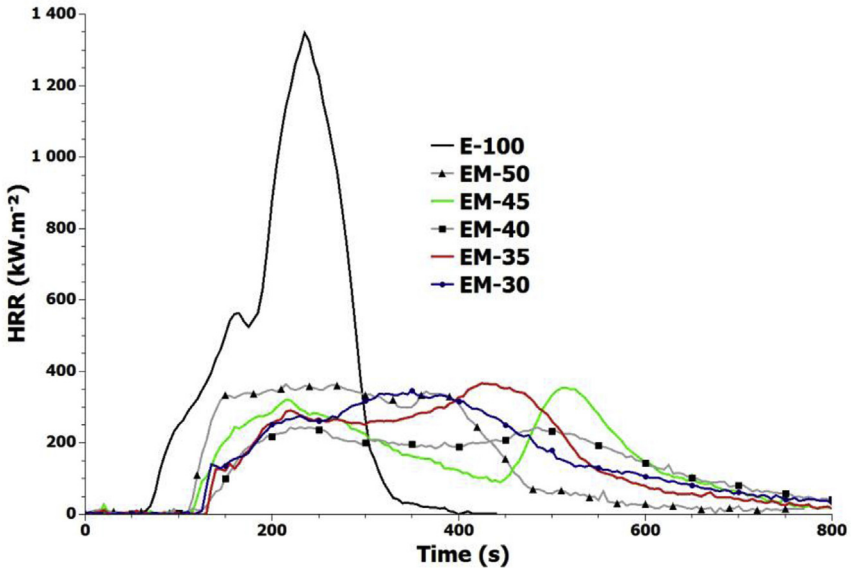

Fig. 5. Heat Release Rate (HRR) curves of EVA, EVA/MDH and EVA/MDH/expanded graphite samples, (Heat flux: 50 kW m^{-2}).

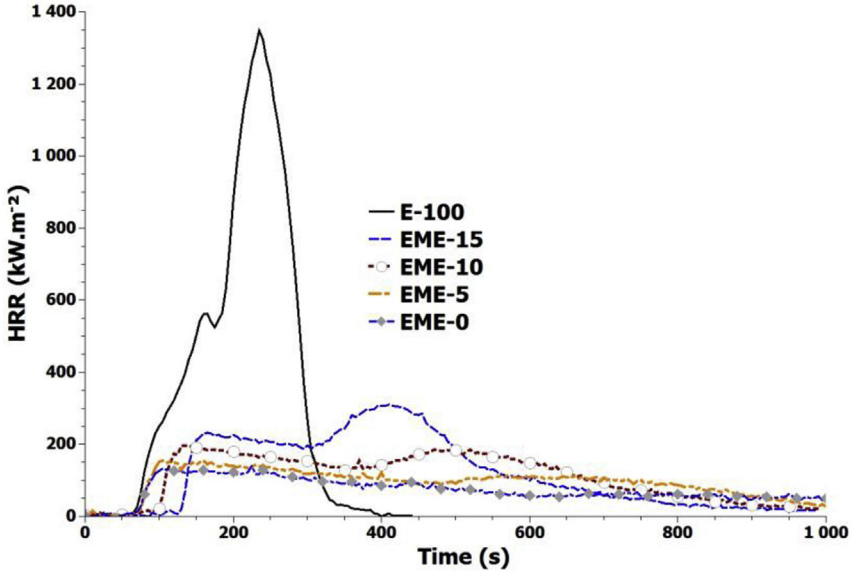

Fig. 6. Heat release rate (HRR) curves of EVA, EVA/MDH/expandable graphite, and EVA/MDH/expanded graphite/expandable graphite samples, (Heat flux: 50 kW m^{-2}).

Table 4
Summary results of cone calorimetry test (* The residue was brittle and it was not possible to measure its thickness).

	1st pHRR ($kW.m^{-2}$)	2^{nd} pHRR ($kW.m^{-2}$)	THR ($MJ.m^{-2}$)	THR ($kJ.g^{-1}$)	TTI (s)	pHRR reduction (%)	TSP ($m^2.m^{-2}$)	Char thickness (mm)
E100	1350	–	158	38.9	65	–	2630	0
EM-50	360	342	116	19.6	110	73.4	2655	-*
EM-45	319	355	119	19.5	115	73.8	2795	9
EM-40	240	242	114	18.7	125	82	2795	16
EM-35	290	366	123	19.6	130	72.8	1535	18
EM-30	341	–	127	20.5	125	74.7	875	20
EME-15	230	309	117	19.9	125	77.2	1075	19
EME-10	197	185	108	18.3	99	85.4	987	25
EME-5	155	–	98	16.8	75	88.5	410	37
EME-0	130	–	79	13.8	75	90.4	190	48

added to EVA can be assigned to the dilution of fuels in gas phase through the endothermic release of water by MDH decomposition. MDH releases 31 wt.% of water and the enthalpy of decomposition is 1450 J g^{-1} [60]. The water release occurs in the same temperature

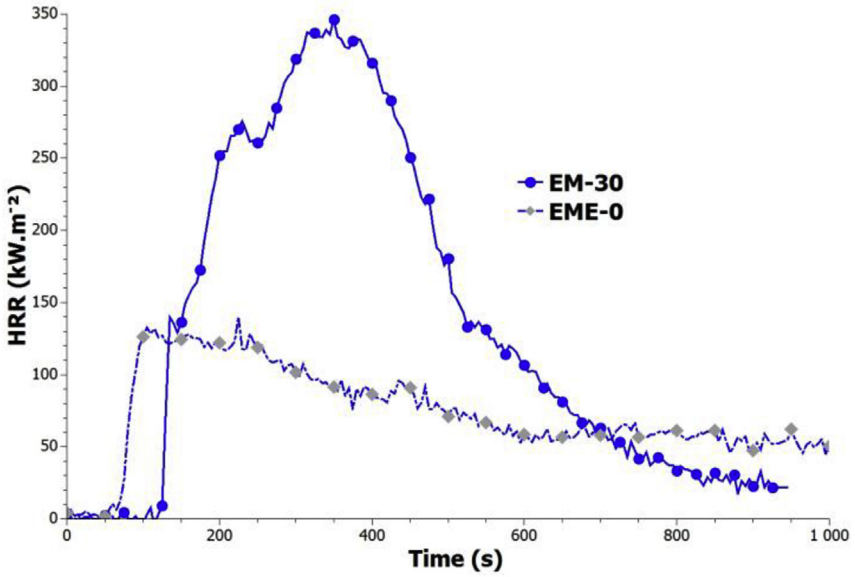

Fig. 7. Comparaison of HRR curves of EM-30 and EME-0 samples.

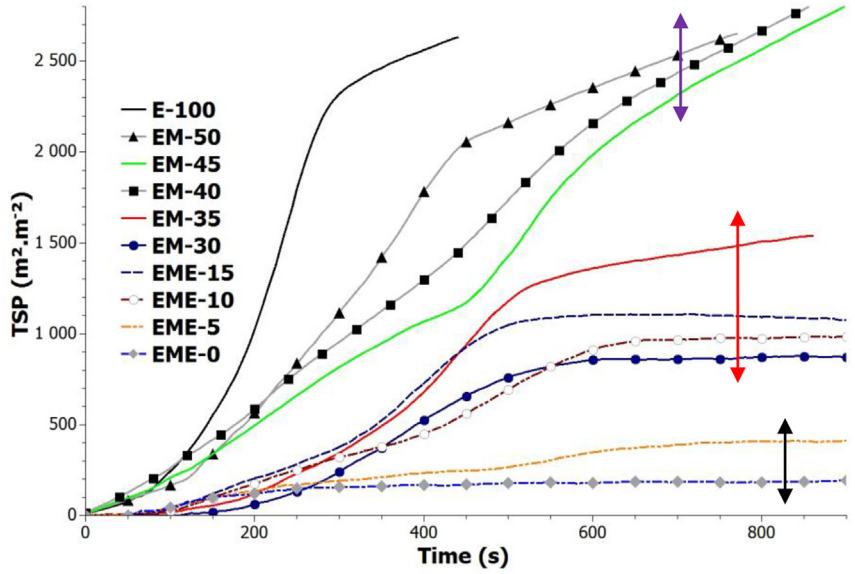

Fig. 8. Total Smoke Production (TSP) curves of all samples, obtained from cone calorimeter test, heat flux: 50 kW m^{-2}.

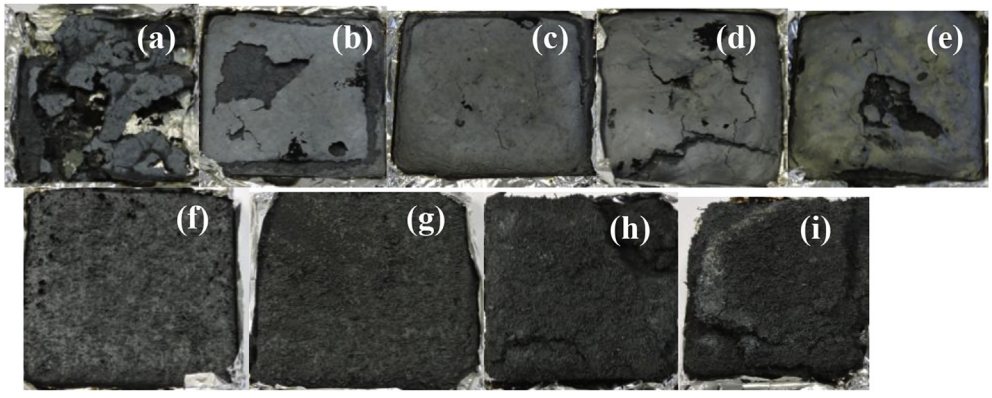

Fig. 9. Pictures of the residues remaining after the cone calorimeter test a) EM-50, b) EM-45, c) EM-40, d) EM-35, e) EM-30, f) EME-15, g) EME-10, h) EME-5, and f) EME-0.

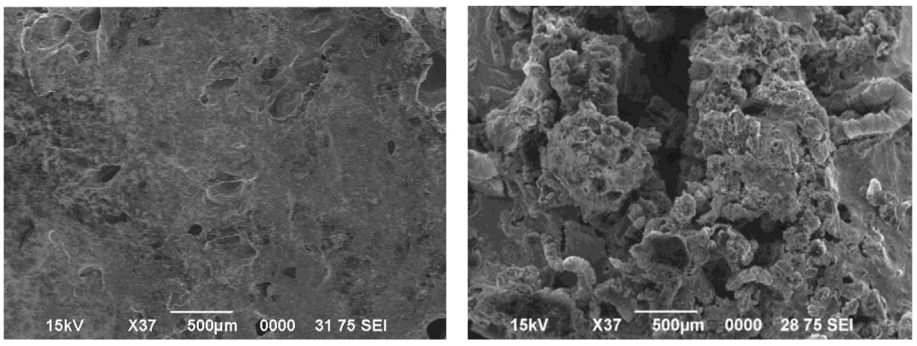

Fig. 10. SEM images of the residues remaining after the cone calorimeter test for EM-40 (a) and EME-10 (b) samples.

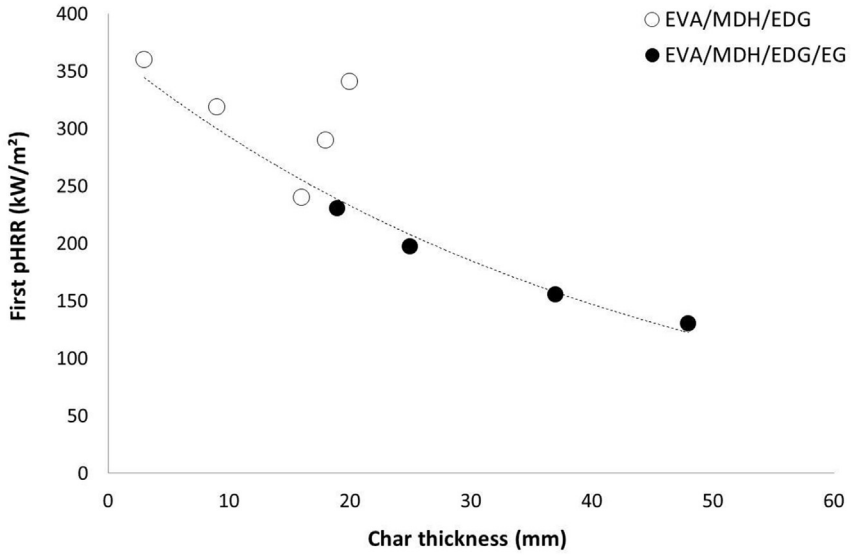

Fig. 11. First pHRR versus char thickness for all samples (excluding E100).

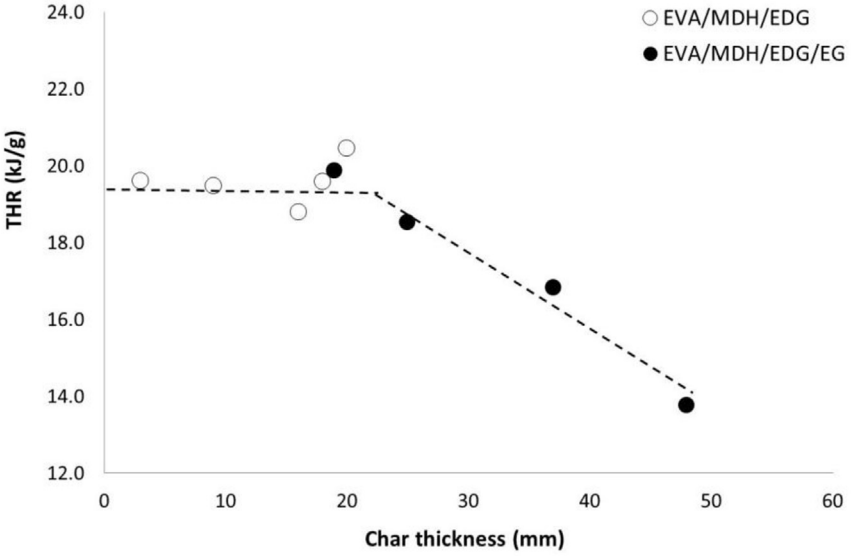

Fig. 12. THR versus char thickness for all samples (excluding E100).

range as the first step of decomposition of EVA (release of acetic acid). Nevertheless, the partial substitution of MDH with EDG delays ignition despite the fact that EDG does not release water. The incorporation of EDG allows a linear increase in thermal

conductivity as shown in Fig. 13. It is well known that a high thermal conductivity promotes a fast heat transfer from the surface to the bulk, limiting the heating rate of the surface [43,61]. Therefore the increase in thermal conductivity allows delaying ignition (Fig. 13). TTI increases from 110 to 130 s when 15 wt.% of EDG are added. TTI decreases slightly with a further increase in EDG, probably because the increase in thermal diffusivity does not balance the decrease in the endothermic release of water.

EG has a different influence on TTI. When EDG is partially replaced with 5 wt.% of EG, the thermal conductivity increases from 1.56 to 1.85 W $m^{-1}.K^{-1}$ (Fig. 15) and TTI remains constant (Fig. 14). A higher amount of EG leads to a decrease in thermal diffusivity and TTI. Even if composites containing 10–20 wt.% of EG have a higher conductivity than EVA/MDH 50/50, their TTI is much lower. When the content of EG is 15–20 wt.%, TTI is close to the TTI of pure EVA. It can therefore be assumed that EG has a strong detrimental effect on time-to-ignition. It is noteworthy that various phenomena may modify the time-to-ignition. For example, higher absorptivity of EG may promote a fast heating rate of the surface composite. The decomposition of EG at low temperature (around 200 °C) may also promote earlier ignition.

High thermal conductivity can delay ignition but promotes a fast heating rate of the bulk leading to an increase in HRR during cone calorimeter test [43]. Nevertheless, the formation of a protective layer during cone calorimeter test also has a strong influence on heat release rate and can avoid a fast decomposition despite a high heat transfer from the surface to the bulk. Residues from cone calorimeter tests were cooled and submitted to heat flux of 50 kW m^{-2}. A thermocouple was used to measure the temperature of the lower surface during the heating (Scheme 2 and Fig. 16). The temperature increases very slowly for EME-0 residue, evidencing the insulating effect of the expanded residue containing 20 wt.% of EG. EME-5 and EME-10 also provide an expanded residue but the temperature increases much faster. After 400 s, the temperature

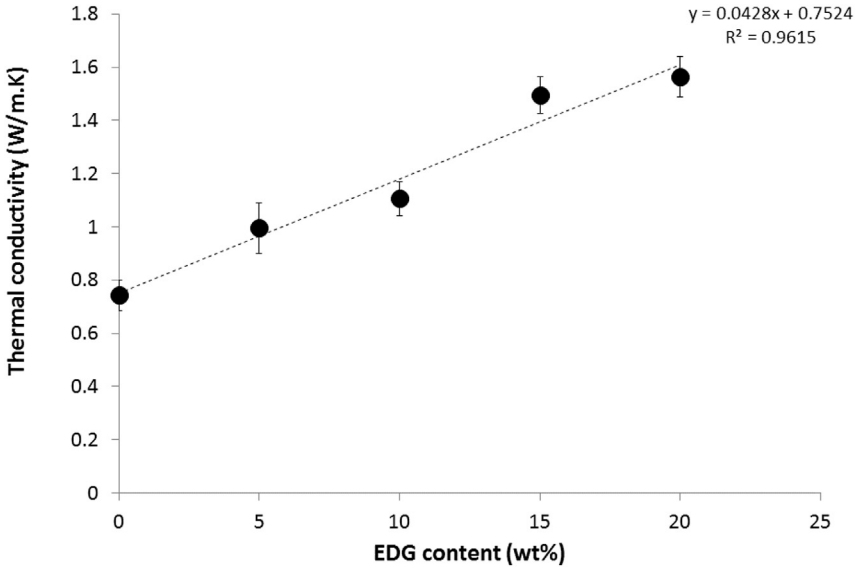

Fig. 13. Thermal conductivity of composites containing MDH and EDG (filler content is fixed to 50 wt.%).

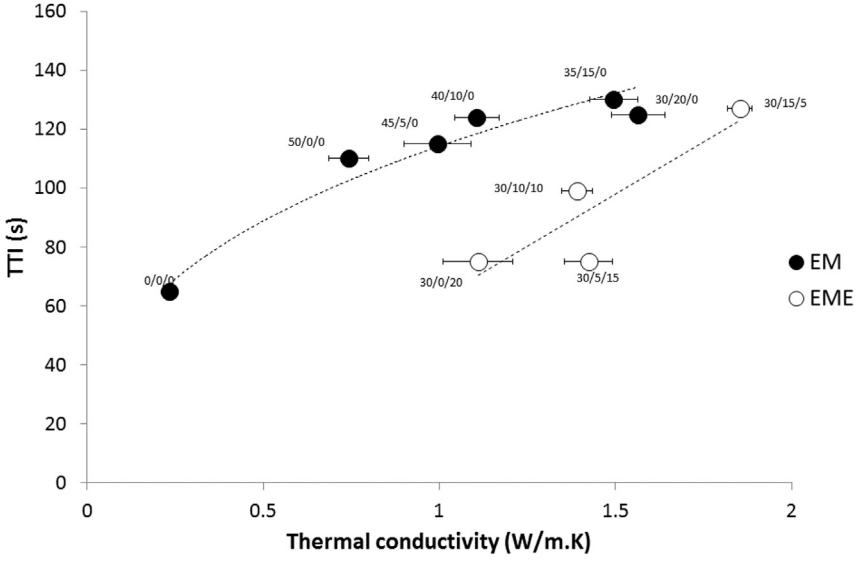

Fig. 14. Time-to-ignition versus thermal conductivity (X/Y/Z corresponds to X wt.% of MDH, Y wt.% of EDG and Z wt.% of EG).

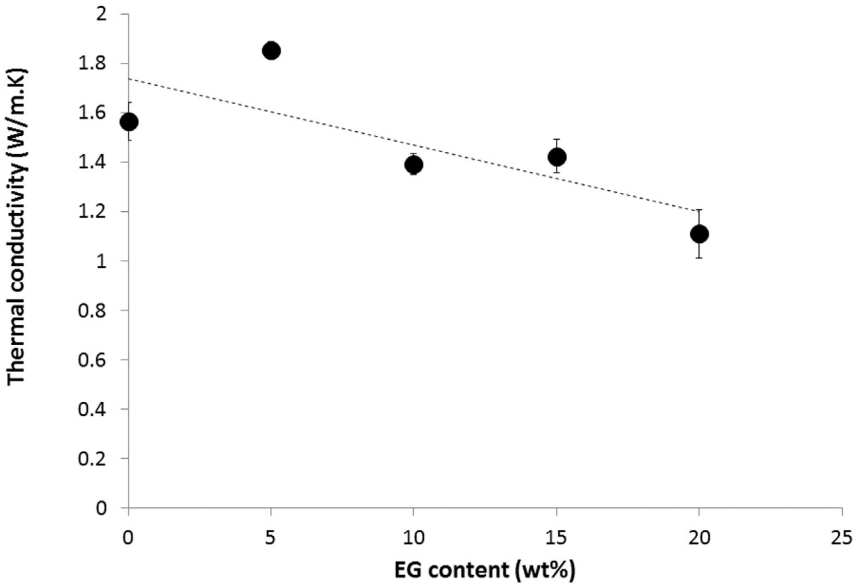

Fig. 15. Thermal conductivity of composites containing MDH, EDG and EG (filler content is fixed to 50 wt.%, MDH content is fixed to 30 wt.%).

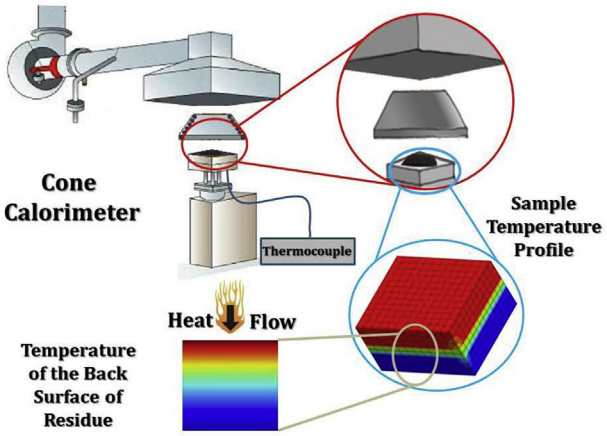

Scheme 2. Experimental setup for the measurement of back surface temperature of residues.

reaches 130 and 160 °C respectively for these two residues, versus only 60 °C for EME-0 residue. The insulating character of the residue may be partially disrupted due to an increase in the thermal conductivity provided by EDG filler. The temperature increases similarly for all EM composites and reaches 140–170 °C after 400 s (as EME-10). It can be observed that the best insulating residues (i.e. EME-0 and EME-5) correspond to the lowest pHRR measured in cone calorimeter test.

4. Conclusion

Magnesium hydroxide, expandable and expanded graphites contribute to improve the flame retardancy of EVA through various modes-of-action. Magnesium hydroxide delays ignition through endothermic release of water diluting fuels in gaseous phase and formation of a mineral layer (magnesium oxide). Nevertheless, this layer is very thin and not effective as insulating barrier. Expandable graphite promotes the formation of an intumescent layer,

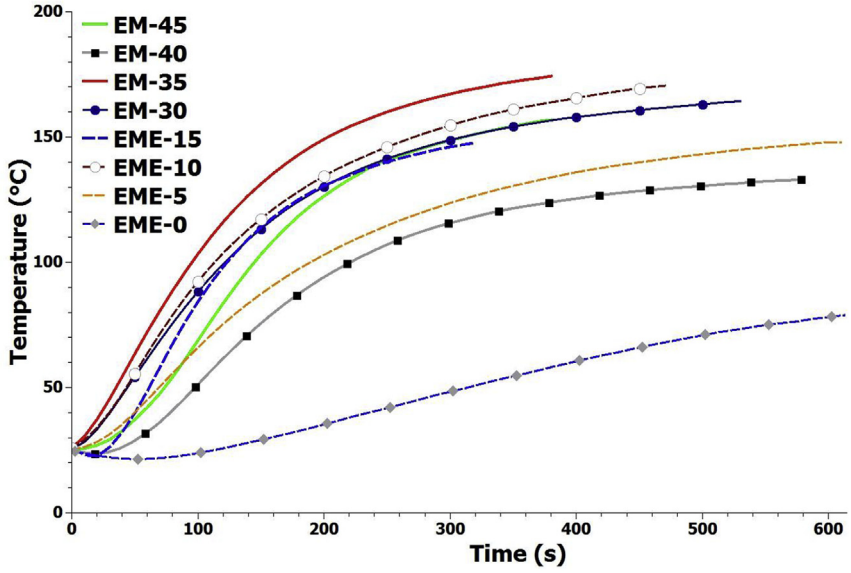

Fig. 16. Temperature of the back surface of residues, obtained from cone calorimeter test (residues were exposed to heat flux of 50 kW m^{-2}).

significantly reducing the peak of heat release rate, the total heat release and the smoke production. However, ignition occurs earlier in the presence of a moderate content of expandable graphite. Finally, expanded graphite contributes to delay ignition thanks to its high thermal conductivity. It also improves char thickness when combining with magnesium hydroxide, even if it is less effective than expandable graphite from this point of view. The formation of a char layer together with magnesium hydroxide and/or expandable graphite further avoids the fact that the fast heating of the sample bulk leads to a fast degradation rate (and therefore a high heat release rate) during the second part of the test. The analysis of cone calorimeter results shows that char thickness is highly correlated to heat release, including just after ignition. Indeed, the correlations found between the thickness of the residue and the first peak of heat release rate were quite consistent. From a performance point of view, the combination of these three fillers can be considered as synergistic, i.e. an optimum composition (ratio between expanded and expandable graphite), can be found to reach the best flame retardancy performances. This does not mean that there is synergy from a mechanistic point of view. The best combination may be close to 30 wt.% of Magnesium hydroxide, 10 wt.% of expanded graphite and 10 wt.% of expandable graphite for a total filler content of 50 wt.%. Nevertheless, this optimum composition may depend on the considered fire test. Finally, it can be assumed that the competitiveness between expanded and expandable graphites to decrease of heat release rate and/or increase of time-to-ignition can be monitored using an optimum composition.

Funding

This research did not receive any specific grant from funding agencies in the public, commercial, or not-for-profit sectors.

Acknowledgements

The authors wish to thank the technological platform “Plastinnov” and Arthur Joswik, at the University of Lorraine for their support in the preparation of samples and fire tests. The authors also gratefully acknowledge Alain Diaz for the preparation of some samples and Jean-Claude Roux for SEM observations.

References

[1] A.M. Henderson, Ethylene-vinyl acetate (EVA) copolymers: a general review, IEEE Electr. Insul. Mag. 9 (1) (1993) 30–38.

[2] Global ethylene vinyl acetate market 2016–2020. http://www.researchandmarkets.com, June 2016.

[3] A. Riva, G. Camino, L. Fomperie, P. Amigouet, Fire retardant mechanism in intumescent ethylene vinyl acetate compositions, Polym. Degrad. Stab. 82 (2) (2003) 341–346.

[4] X. Wang, E.N. Kalali, J.-T. Wan, D.-Y. Wang, Carbon-family materials for flame retardant polymeric materials, Prog. Polym. Sci. 69 (2017) 22–46.

[5] A. Szép, A. Szabó, N. Tóth, P. Anna, G. Marosi, Role of montmorillonite in flame retardancy of ethylene–vinyl acetate copolymer, Polym. Degrad. Stab. 91 (3) (2006) 593–599.

[6] S. Duquesne, C. Jama, M. Le Bras, R. Delobel, P. Recourt, J. Gloaguen, Elaboration of EVA–nanoclay systems-characterization, thermal behaviour and fire performance, Compos Sci. Techno 63 (8) (2003) 1141–1148.

[7] J. Zilberman, T.R. Hull, D. Price, G.J. Milnes, F. Keen, Flame retardancy of some ethylene–vinyl acetate copolymer-based formulations, Fire Mater 24 (3) (2000) 159–164.

[8] G. Camino, R. Sgobbi, A. Zaopo, S. Colombier, C. Scelza, Investigation of flame retardancy in EVA, Fire Mater 24 (2) (2000) 85–90.

[9] G. Beyer, Flame retardant properties of EVA-nanocomposites and improvements by combination of nanofillers with aluminium trihydrate, Fire Mater 25 (5) (2001) 193–197.

[10] D. Gnanasekaran, P.H. Massinga, W.W. Focke, A Detailed Review on Behavior of Ethylene-Vinyl Acetate Copolymer Nanocomposite Materials. Materials Behavior: Research Methodology and Mathematical Models, Apple Academic Press, 2015, pp. 89–123.

[11] L. Clerc, L. Ferry, E. Leroy, J.-M. Lopez-Cuesta, Influence of talc physical properties on the fire retarding behaviour of (ethylene–vinyl acetate copolymer/magnesium hydroxide/talc) composites, Polym. Degrad. Stab. 88 (3) (2005) 504–511.

[12] Y. Arao, Flame Retardancy of Polymer Nanocomposite. Flame Retardants, Springer, 2015, pp. 15–44.

[13] M. Muller, S. Bourbigot, S. Duquesne, R.A. Klein, G. Giannini, C.I. Lindsay, Measurement and investigation of intumescent char strength: application to polyurethanes, J. Fire Sci. 31 (4) (2013) 293–308.

[14] T. Mariappan, Recent developments of intumescent fire protection coatings for structural steel: a review, J. Fire Sci. 34 (2) (2016) 120–163.

[15] British Standard BS EN 50200, Method of Test for Resistance to Fire of Unprotected Small Cables for Use in Emergency Circuits, British Standard Institution, 2006.

[16] S. Hamdani-Devarennes, A. Pommier, C. Longuet, J.-M. Lopez-Cuesta, F. Ganachaud, Calcium and aluminium-based fillers as flame-retardant additives in silicone matrices II. Analyses on composite residues from an industrial-based pyrolysis test, Polym. Degrad. Stab. 96 (9) (2011) 1562–1572.

[17] F. Carpentier, S. Bourbigot, M. Le Bras, R. Delobel, M. Foulon, Charring of fire retarded ethylene vinyl acetate copolymer-magnesium hydroxide/zinc borate formulations, Polym. Degrad. Stab. 69 (1) (2000) 83–92.

[18] F. Carpentier, S. Bourbigot, M. Le Bras, R. Delobel, Rheological investigations in fire retardancy: application to ethylene-vinyl-acetate copolymer–magnesium hydroxide/zinc borate formulations, Polym. Int. 49 (10) (2000) 1216–1221.

[19] S. Bourbigot, M. Le Bras, R. Leeuwendal, K.K. Shen, D. Schubert, Recent advances in the use of zinc borates in flame retardancy of EVA, Polym. Degrad. Stab. 64 (3) (1999) 419–425.

[20] A. Durin-France, L. Ferry, J.M. Lopez Cuesta, A. Crespy, Magnesium hydroxide/zinc borate/talc compositions as flame-retardants in EVA copolymer, Polym. Int. 49 (10) (2000) 1101–1105.

[21] C. Hoffendahl, G. Fontaine, S. Duquesne, F. Taschner, M. Mezger, S. Bourbigot, The combination of aluminum trihydroxide (ATH) and melamine borate (MB) as fire retardant additives for elastomeric ethylene vinyl acetate (EVA), Polym. Degrad. Stab. 115 (2015) 77–88.

[22] A. Cardelli, G. Ruggeri, M. Calderisi, O. Lednev, C. Cardelli, E. Tombari, Effects of poly (dimethylsiloxane) and inorganic fillers in halogen free flame retardant poly (ethylene-co-vinyl acetate) compound: a chemometric approach, Polym. Degrad. Stab. 97 (12) (2012) 2536–2544.

[23] G. Beyer, Flame retardancy of nanocomposites based on organoclays and carbon nanotubes with aluminium trihydrate, Polym. Adv. Techno 17 (4) (2006) 218–225.

[24] A. Szep, A. Szabo, N. Toth, P. Anna, G. Marosi, Role of montmorillonite in flame retardancy of ethylene-vinyl acetate copolymer, Polym. Degrad. Stab. 91 (3) (2006) 593–599.

[25] L. Haurie, A.I. Fernández, J.I. Velasco, J.M. Chimenos, J.-M.L. Cuesta, F. Espiell, Thermal stability and flame retardancy of LDPE/EVA blends filled with synthetic hydromagnesite/aluminium hydroxide/montmorillonite and magnesium hydroxide/aluminium hydroxide/montmorillonite mixtures, Polym. Degrad. Stab. 92 (6) (2007) 1082–1087.

[26] M. Cárdenas, D. García-López, I. Gobernado-Mitre, J. Merino, J. Pastor, JdD. Martínez, et al., Mechanical and fire retardant properties of EVA/clay/ATH nanocomposites–Effect of particle size and surface treatment of ATH filler, Polym. Degrad. Stab. 93 (11) (2008) 2032–2037.

[27] F. Laoutid, P. Gaudon, J.-M. Taulemesse, J.L. Cuesta, J. Velasco, A. Piechaczyk, Study of hydromagnesite and magnesium hydroxide based fire retardant systems for ethylene–vinyl acetate containing organo-modified montmorillonite, Polym. Degrad. Stab. 91 (12) (2006) 3074–3082.

[28] Y. Zhang, Y. Hu, L. Song, J. Wu, S. Fang, Influence of Fe-MMT on the fire retarding behavior and mechanical property of (ethylene-vinyl acetate copolymer/magnesium hydroxide) composite, Polym. Adv. Technol. 19 (8) (2008) 960–966.

[29] J. Zhang, J. Hereid, M. Hagen, D. Bakirtzis, M. Delichatsios, A. Fina, A. Castrovinci, G. Camino, F. Samyn, S. Bourbigot, Effects of nanoclay and fire retardants on fire retardancy of a polymer blend of EVA and LDPE, Fire Saf. J. 44 (4) (2009) 504–513.

[30] B. Girardin, G. Fontaine, S. Duquesne, M. Försth, S. Bourbigot, Measurement of kinetics and thermodynamics of the thermal degradation for flame retarded materials: application to EVA/ATH/NC, J. Anal. Appl. Pyrolysis 124 (2017) 130–148.

[31] R. Sonnier, A. Viretto, L. Dumazert, M. Longerey, S. Buonomo, B. Gallard, C. Longuet, F. Cavodeau, R. Lamy, A. Freitag, Fire retardant benefits of combining aluminum hydroxide and silica in ethylene-vinyl acetate copolymer (EVA), Polym. Degrad. Stab. 128 (2016) 228–236.

[32] F. Cavodeau, R. Sonnier, B. Otazaghine, J.-M. Lopez-Cuesta, C. Delaite, Ethylene-vinyl acetate copolymer/aluminium trihydroxide composites: a new method to predict the barrier effect during cone calorimeter tests, Polym. Degrad. Stab. 120 (2015) 23–31.

[33] F. Cavodeau, B. Otazaghine, R. Sonnier, J.-M. Lopez-Cuesta, C. Delaite, Fire retardancy of ethylene-vinyl acetate composites–Evaluation of synergistic effects between ATH and diatomite fillers, Polym. Degrad. Stab. 129 (2016) 246–259.

[34] M. Fu, B. Qu, Synergistic flame retardant mechanism of fumed silica in ethylene-vinyl acetate/magnesium hydroxide blends, Polym. Degrad. Stab. 85 (1) (2004) 633–639.

[35] L. Ye, P. Ding, M. Zhang, B. Qu, Synergistic effects of exfoliated LDH with some

halogen-free flame retardants in LDPE/EVA/HFMH/LDH nanocomposites, J. Appl. Polym. Sci. 107 (6) (2008) 3694–3701.
[36] L. Ye, Q. Wu, B. Qu, Synergistic effects and mechanism of multiwalled carbon nanotubes with magnesium hydroxide in halogen-free flame retardant EVA/MH/MWNT nanocomposites, Polym. Degrad. Stab. 94 (5) (2009) 751–756.
[37] Z. Li, B. Qu, Flammability characterization and synergistic effects of expandable graphite with magnesium hydroxide in halogen-free flame-retardant EVA blends, Polym. Degrad. Stab. 81 (3) (2003) 401–408.
[38] X.Y. Pang, M.Q. Weng, Preparation of expandable graphite composite under the auxiliary intercalation of Zinc sulfate and its flame retardancy for ethylene/vinyl acetate copolymer, Int. J. ChemTech Res. 6 (2) (2014) 1291–1298.
[39] X.Y. Pang, Y. Tian, M.Q. Weng, Preparation of expandable graphite with silicate assistant intercalation and its effect on flame retardancy of ethylene vinyl acetate composite, Polym. Compos. 36 (8) (2015) 1407–1416.
[40] X. Wu, L. Wang, C. Wu, G. Wang, P. Jiang, Flammability of EVA/IFR (APP/PER/ZB system) and EVA/IFR/synergist (CaCO3, NG, and EG) composites, J. Appl. Polym. Sci. 126 (6) (2012) 1917–1928.
[41] M. Mochane, A. Luyt, The effect of expanded graphite on the thermal stability, latent heat, and flammability properties of EVA/wax phase change blends, Polym. Eng. Sci. 55 (6) (2015) 1255–1262.
[42] A. Laachachi, N. Burger, K. Apaydin, R. Sonnier, M. Ferriol, Is expanded graphite acting as flame retardant in epoxy resin? Polym. Degrad. Stab. 117 (2015) 22–29.
[43] P. Patel, T.R. Hull, A.A. Stec, R.E. Lyon, Influence of physical properties on polymer flammability in the cone calorimeter, Polym. Adv. Technol. 22 (7) (2011) 1100–1107.
[44] B. Dittrich, K.-A. Wartig, D. Hofmann, R. Mülhaupt, B. Schartel, Flame retardancy through carbon nanomaterials: carbon black, multiwall nanotubes, expanded graphite, multi-layer graphene and graphene in polypropylene, Polym. Degrad. Stab. 98 (8) (2013) 1495–1505.
[45] B. Dittrich, K.-A. Wartig, R. Mülhaupt, B. Schartel, Flame-retardancy properties of intumescent ammonium poly(phosphate) and mineral filler magnesium hydroxide in combination with graphene, Polymers 6 (11) (2014) 2875–2895.
[46] https://hcc.hanwha.co.kr/download/1316_eng.pdf.
[47] R.G. Berman, T.H. Brown, Heat capacity of minerals in the system Na_2O-K_2O-CaO-MgO-FeO-Fe_2O_3-Al_2O_3-SiO_2-TiO_2-H_2O-CO_2: representation, estimation, and high temperature extrapolation, Contrib. Mineral. Petr 89 (2–3) (1985) 168–183.
[48] Y. Ding, G. Zhang, H. Wu, B. Hai, L. Wang, Y. Qian, Nanoscale magnesium hydroxide and magnesium oxide powders: control over size, shape, and structure via hydrothermal synthesis, Chem. Mater 13 (2) (2001) 435–440.
[49] J. Lenża, M. Sozańska, H. Rydarowski, Methods for limiting the flammability of high-density polyethylene with magnesium hydroxide, in: A. Tiwari, B. Raj (Eds.), Reactions and Mechanisms in Thermal Analysis of Advanced Material, John Wiley & Sons Inc, 2015.
[50] W. Mhike, I.V. Ferreira, J. Li, S.I. Stoliarov, W.W. Focke, Flame retarding effect of graphite in rotationally molded polyethylene/graphite composites, J. Appl. Polym. Sci. 132 (7) (2015) 41472–41483.
[51] I. Tavman, Y. Aydogdu, M. Kök, A. Turgut, A. Ezan, Measurement of heat capacity and thermal conductivity of HDPE/expanded graphite nanocomposites by differential scanning calorimetry, Arch. Mater Sci. Eng. 50 (2011) 56–60.
[52] W.W. Focke, H. Muiambo, W. Mhike, H.J. Kruger, O. Ofosu, Flexible PVC flame retarded with expandable graphite, Polym. Degrad. Stab. 100 (2014) 63–69.
[53] Z. Wang, E. Han, KeW. Influence of expandable graphite on fire resistance and water resistance of flame-retardant coatings, Corros. Sci. 49 (2007) 2237–2253.
[54] D.K. Chattopadhyay1, D.C. Webster, Thermal stability and flame retardancy of polyurethanes, Prog. Polym. Sci. 34 (2009) 1068–1133.
[55] M. Zanetti, T. Kashiwagi, L. Falqui, G. Camino, Cone calorimeter combustion and gasification studies of polymer layered silicate nanocomposites, Chem. Mater 14 (2) (2002) 881–887.
[56] M.C. Costache, D.D. Jiang, C.A. Wilkie, Thermal degradation of ethylene-vinyl acetate coplymer nanocomposites, Polymer 46 (2005) 6947–6958.
[57] B. Wang, X. Wang, Y. Shi, G. Tang, Q. Tang, L. Song, Y. Hu, Effect of vinyl acetate content and electron beam irradiation on the flame retardancy, mechanical and thermal properties of intumescent flame retardant ethylene-vinyl acetate copolymer, Radiat. Phys. Chem. 81 (3) (2012) 308–315.
[58] B. Schartel, T.R. Hull, Development of fire-retarded materials-Interpretation of cone calorimeter data, Fire Mater 31 (5) (2007) 327–354.
[59] L. Qian, F. Feng, S. Tang, Bi-phase flame-retardant effect of hexa-phenoxy-cyclotriphosphazene on rigid polyurethane foams containing expandable graphite, Polymer 55 (2014) 95–101.
[60] R. Rothon, P. Hornsby, Flame retardant effects of magnesium hydroxide, Polym. Degrad. Stab. 54 (2–3) (1996) 383–385.
[61] T. Kashiwagi, E. Grulke, J. Hilding, K. Groth, R. Harris, K. Butler, J. Shields, S. Kharchenko, J. Douglas, Thermal and flammability properties of polypropylene/carbon nanotube nanocomposites, Polymer 45 (12) (2004) 4227–4239.